

# In-situ Synchrotron X-ray diffraction Volcanic Ash Infiltration Studies on High Temperature Ceramic Coatings

Zachary Stein\*

Embry-Riddle Aeronautical University, Daytona Beach, FL, 32114, USA

Peter Kenesei<sup>†</sup>, Jun-Sang Park<sup>†</sup>, Jonathan Almer<sup>†</sup> Advanced Photon Source, Argonne National Laboratory, Lemont, IL 60439, USA

Uwe Schulz<sup>‡</sup>, Ravisankar Naraparaju<sup>‡</sup>
German Aerospace Center, 51147 Cologne, Germany

Seetha Raghavan<sup>§</sup> *Embry-Riddle Aeronautical University, Daytona Beach, FL 32114, USA* 

Calcium-magnesium-alumino-silicate (CMAS) particulates, such as sand or volcanic ash (VA), are ingested by aero-engines and negatively interact and degrade high temperature ceramic coatings. These ceramic thermal barrier coatings (TBCs) are used to protect temperature sensitive metallic components, such as turbine blades, from melting due to the extreme temperatures of the hot gas streams formed from the combustor of the engine. In this work, in-situ synchrotron X-ray diffraction measurements were used to capture the interaction and subsequent degradation of a 7 wt% yttria-stabilized zirconia TBC from a VA CMAS composition. In-situ methods have the ability to a greater insight into the mechanisms dominating infiltration as well as capture data regarding the interactions of CMAS and the TBC while in a molten state and upon CMAS solidification while in representative environmental conditions in a controlled laboratory setting. Changes in the bi-axial e11 and e22 strains as well as the formation of new rings, indicative of VA and 7YSZ interactions during infiltration. These results demonstrate the capabilities to capture highly resolved CMAS and coating interactions during operation which is important for capturing, evaluating, and elucidating potential CMAS mitigation strategies.

<sup>\*</sup>Graduate Student, Aerospace Engineering, Embry-Riddle Aeronautical University, Daytona Beach, FL, 32114, USA

<sup>&</sup>lt;sup>†</sup>Beamline Scientist, Advanced Photon Source, Argonne National Laboratory, Lemont, IL 60439, USA

<sup>\*</sup>Material Research Scientist, Institute of Materials Research, German Aerospace Center, 51147 Cologne, Germany

<sup>§</sup>Professor, Aerospace Engineering, Embry-Riddle Aeronautical University, Daytona Beach, FL 32114, USA, AIAA Associate Fellow, raghavs3@erau.edu

## I. Nomenclature

7YSZ = 7 wt% (4 mol%) Yttria Stabilized Zirconia CMAS = Calcium-magnesium-alumino-silicate

TBC = Thermal barrier coating

VA = Volcanic Ash XRD = X-ray Diffraction

#### II. Introduction

High temperature ceramic coatings insulate underlying superalloy metallic components from the hot gas streams within the gas turbine engines used for aerospace applications. These ceramic coatings, known as thermal barrier coatings (TBCs), are coupled with additionally cooling methods to allow for higher operating temperatures and for greater engine efficiency. TBCs on turbine blades comprise of around 150 - 200  $\mu$ m thick ceramic top coat layer of 7 wt% yttria-stabilized zirconia (7YSZ) with a typical thermal gradient of about 150 - 200  $\mu$ C through the thickness of the coating [1–3].

For turbine blades, electron-beam physical vapor deposition (EB-PVD) is the typical deposition method for applying TBCs since this method provides a microstructure that exhibits a higher in-plane strain tolerance and lower thermal conductivity, favorable for moving components within aero-engines. The microstructure formed by EB-PVD are of a closed porosity columnar microstructure that forms during deposition, which can be further tailored by modifying the deposition parameters [4, 5].

TBCs are highly susceptible to calcium-magnesium-aluminosilicates (CMAS) particulates, such as sand or volcanic ash (VA), especially during high temperature operation. These particulates are ingested into the engine, becoming molten once reaching the combustor section during operation. These molten particulates flow along the hot gas stream into the turbine section of the engine and deposit onto the surface of the high temperature ceramic coated turbine blades. The CMAS melt begins to infiltrate and attack the TBC, introducing additional residual stresses to the coating and destabilizing the coating. The interactions between the CMAS and TBC greatly increases the risk of premature coating failure through spallation. The infiltration itself is accelerated through capillary effects as a result of the intercolumnar gaps present within EB-PVD coatings [5]. CMAS-related degradation affects the overall durability and lifetime of the coating and therefore also limits the operational capabilities of aircraft operating in highly abundant CMAS regions. To this effect, capturing, monitoring, and elucidating the interdependent infiltration mechanisms and the overall influence of CMAS infiltration on the thermochemical and thermomechanical properties of the coating over time is imperative towards finding ways to mitigate the effects of CMAS-related degradation for in-service coatings and their overall service lifetime without compromising their effectiveness in protecting underlying temperature sensitive components. Previous studies have looked at in-situ behaviors representative of operating conditions and its effects ex-situ as a result of rapidly changing environments for ceramic coatings on their own [6-11]. This study builds upon these previous studies using high-energy X-ray diffraction (XRD) from a synchrotron source, to capture the in-situ effects of CMAS infiltration over the course of an hour before cooling down and allowing for the molten CMAS to solidify similar to what would occur over an operational cycle.

## **III. Experimental Methods**

### A. High Temperature Ceramic Coatings Sample Manufacturing

Within this study, a 7YSZ EB-PVD coating deposited onto a 25.4 mm diameter disc of Rene N5 nickel-based superalloy substrate doped with yttrium with a PtAl bond coat. The substrate is 3 mm thick, bond coat thickness is about 50  $\mu$ m, and 7YSZ thickness, on average, is about 150  $\mu$ m. This sample was aged through 300 thermal cycles in an open-air furnace with each cycle performed consisting of 1 hour of hot time at 1100°C followed by a 10 minute cool time with fan-assisted cooling. The TBC system's temperature was approximately 100°C at the end of the cool time. To prepare this sample for X-ray transmission measurements, the sample was center sliced to a width of 2.5 mm with a diamond saw, rinsed with cold deionized water and dried with compressed air with no visible signs of spallation after slicing. This thickness was determined to be optimal for X-ray transmission measurement while minimizing stress-relieving effects from slicing. The methodology from this sample preparation work is further described in previous studies [12, 13].

## **B. VA Fabrication & Composition**

The volcanic ash used within this study was collected from a site corresponding to the Eyjafjallajökull volcano located in Iceland (in mol.%: 49.7% SiO-2, 12.5% CaO, 6.1% MgO, 7.4% Al<sub>2</sub>O-3, 17.6% FeO, 4.3% TiO<sub>2</sub>, 2.0% Na<sub>2</sub>O, & 0.4% K<sub>2</sub>O). This volcanic ash (VA) composition was selected due to its initial amorphous state and having a relatively lower melting point at 1150°C as compared to other CMAS compositions. The melting point of the VA used within this study was determined through differential scanning calorimetry and is described and compared with other CMAS and volcanic ash compositions in greater detail in [14].

## C. In-situ synchrotron XRD Experimental Parameters

High-energy XRD measurements were performed at the 1-ID beamline of the Advanced Photon Source at Argonne National Laboratory. The incident beam size was 200  $\mu$ m horizontally by 15  $\mu$ m vertically with a beam energy of 59.732 keV and a probed volume of 0.0563 mm³. High-energy XRD from a synchrotron was selected due to its high spatial resolutions and fast data acquisition. The sliced sample was placed ontop of an Inconel rod sample holder inside of an IR furnace with four heating lamps. A K-type thermocouple was placed in between top of the sample holder and the bottom of the Rene N5 substrate of the sample to track and control the temperature of the furnace. The incident beam impinged onto the sample and diffracted full Debye-Scherrer rings that were captured on a GE-41RT 2048 x 2048 pixel area detector with a sample to detector distance of roughly 2200 mm. CeO<sub>2</sub> powder was used to calibrate the instrument. Data was collected with an exposure time of 0.3 s. and was taken across the thickness of the 7YSZ layer, bond coat, and slightly into the substrate.

#### D. VA Infiltration Parameters & Thermal Cycle Profile

The VA was measured, mixed with deionized water to form a paste, and applied to the center of the sliced sample in a 5 x 2.5 mm<sup>2</sup> area (H x W) at a concentration of 10 mg/cm<sup>2</sup> so that the incident beam would easily travel only through the VA-exposed and infiltrated parts of the coating. The sample then sat to allow for the deionized water to fully evaporate, leaving behind only the VA deposited onto the surface of the coating. A thermal profile used within this study is shown in Fig. 1 for data acquisition of roughly one cycle.

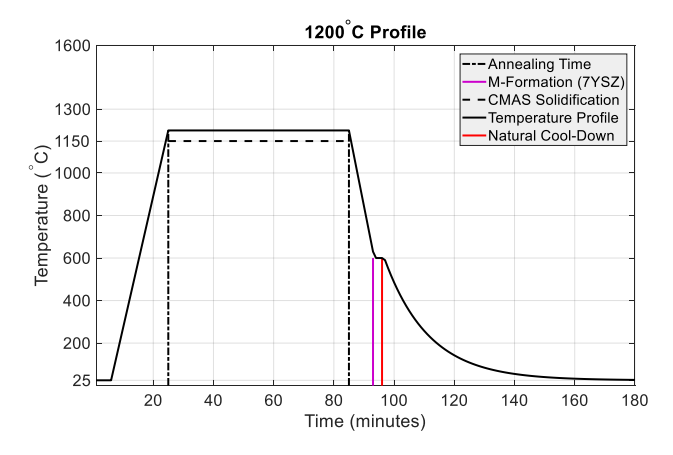


Fig. 1 The 1 hour VA infiltration Thermal Profile used within this experiment

The sample started at room temperature and brought to 1200°C with a ramp rate of 40 K/min, well above the 1150°C melting point of the VA to ensure any discrepancies in the thermocouple were negated. The VA was allowed to infiltrate and interact with the sample for 1 hour at 1200°C before ramping down at controlled rate of 40 K/min until reaching 630°C. The sample was then held here for a brief moment to allow for data to be collected above and below 600°C, which is roughly the temperature in which the monoclinic phase of ZrO<sub>2</sub> is formed. From 600°C, the IR furance was turned off and the sample was naturally cooled until reaching room temperature. Data was collected at room temperature before infiltration, throughout the duration of the thermal profile from ramp up, the 1 hour hold at 1200°C, throughout ramp down, and at roughly room temperature, 83°C specifically, during cool down.

## **IV. Results & Discussion**

Fig. 2 shows a fourth of three full Debye-Scherrer XRD rings collected at the surface of the 7YSZ layer at the VA/7YSZ interface at various points during the thermal cycle.

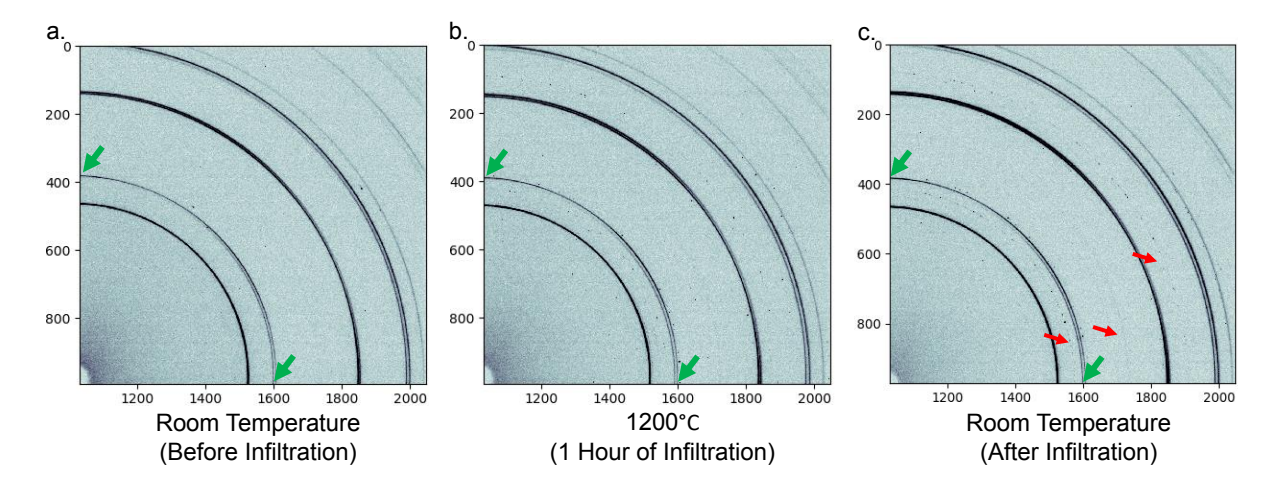


Fig. 2 The Debye-Scherrer rings at the top of the 7YSZ layer at (a) room temperature before infiltration, (b) 1200°C after 1 hour of infiltration, and (c) room temperature after infiltration. The green arrows follows a doublet of 7YSZ rings, with a d-spacing of roughly 2.57 and 2.56 Å, and the expansion and compression of these rings throughout the thermal cycle; meanwhile, the red arrows show new rings that form in the room temperature measurements after infiltration

Only a fourth of these rings are shown in Fig. 2 as to more easily depict the subtle changes in the rings due to changes in the bi-axial strains. These changes are seen through the expansion or contraction of these rings relative to their pixel location shown on both the x- and y-axis. The green arrow on the rings depicts this expansion and contraction for a 7YSZ doublet located around 2.57 and 2.56 Å. What can be observed following this doublet is a contraction at Fig. 2(b) 1200°C relative to the room temperature measurements 2(a) before and 2(c) after infiltration. Similarly, an expansion of the doublet is observed at 2(b) 1200°C relative to the room temperature measurements 2(a) before and 2(c) after infiltration. The x-direction refers to e11 strain while the y-direction refers to the e22 strain. Since 7YSZ is deposited through EB-PVD methods at high temperatures, it is expected that the coating would experience some relaxation at high temperatures and hold some residual strains at cooler temperature, explaining the changes in the e11 and e22 strains going from room temperature to 1200°C and back to room temperature.

The red arrows in Fig. 2(c) highlight the faint new rings that have appeared only after infiltration. This suggests that these rings are the result of VA interacting with the 7YSZ, however further work is required to identify these rings. Overall, this shows that the VA successfully infiltrated into the coating and had some reactions. Physical observations were also made before and after infiltration with the volcanic ash initially deposited as a grey color and turning into a reddish glass after 1 hour of infiltration upon cooling down.

## V. Conclusion

Exposure to CMAS, such as VA used within this study, degrades high temperature ceramic coatings that are essential to protect underlying superalloy metallic components from melting and causing catastrophic engine failure during operation for aircraft gas turbine engines. Replicating operation conditions these coatings experience when exposed to CMAS in a controlled laboratory setting is vital to capture and elucidate the transitory interactions between the CMAS and ceramic coating. The work presented has demonstrated a way to capture in-situ CMAS infiltration through synchrotron XRD showing changes in the e11 and e22 strains as well as additional rings, suggesting the formation of a new crystalline phase as a result of the interaction between the VA and 7YSZ coating. This in-situ synchrotron XRD setup is not limited to volcanic ash or 7YSZ coatings and can be applied to see other in-situ characteristics and properties of novel coatings and their interactions with other CMAS compositions, providing a greater depth of information for potential mitigation strategies against CMAS infiltration. An excellent example of this would be to capture the formation

rate of the reactionary layer that forms between the interaction of CMAS and gadolinium zirconate coatings.

# Acknowledgments

This research used resources of the Advanced Photon Source, a U.S. Department of Energy (DOE) Office of Science User Facility operated for the DOE Office of Science by Argonne National Laboratory under Contract No. DE-AC02-06CH11357. Funding: This material is based upon work supported by National Science Foundation grant OISE 1952523, Fulbright Academic Grant, and the Department of Defense (DoD) through the National Defense Science & Engineering Graduate (NDSEG) Fellowship Program.

## References

- [1] Miller, R. A., "Thermal barrier coatings for aircraft engines: history and directions," *Journal of thermal spray technology*, Vol. 6, No. 1, 1997, pp. 35–42.
- [2] Knipe, K., Manero II, A., Siddiqui, S. F., Meid, C., Wischek, J., Okasinski, J., Almer, J., Karlsson, A. M., Bartsch, M., and Raghavan, S., "Inside the Engine Environment–Synchrotrons Reveal Secrets of High-Temperature Ceramic Coatings," *American Ceramic Society Bulletin*, Vol. 94, No. 1, 2015, p. 22.
- [3] Sobhanverdi, R., and Akbari, A., "Porosity and microstructural features of plasma sprayed Yttria stabilized Zirconia thermal barrier coatings," *Ceramics International*, Vol. 41, No. 10, 2015, pp. 14517–14528.
- [4] Schulz, U., Saruhan, B., Fritscher, K., and Leyens, C., "Review on advanced EB-PVD ceramic topcoats for TBC applications," *International journal of applied ceramic technology*, Vol. 1, No. 4, 2004, pp. 302–315.
- [5] Naraparaju, R., Hüttermann, M., Schulz, U., and Mechnich, P., "Tailoring the EB-PVD columnar microstructure to mitigate the infiltration of CMAS in 7YSZ thermal barrier coatings," *Journal of the European Ceramic Society*, Vol. 37, No. 1, 2017, pp. 261–270.
- [6] Knipe, K., Manero, A., Siddiqui, S. F., Meid, C., Wischek, J., Okasinski, J., Almer, J., Karlsson, A. M., Bartsch, M., and Raghavan, S., "Strain response of thermal barrier coatings captured under extreme engine environments through synchrotron X-ray diffraction," *Nature communications*, Vol. 5, No. 1, 2014, pp. 1–7.
- [7] Diaz, R., Mossaddad, M., Bozan, A., Raghavan, S., Almer, J., Okasinski, J., Palaez-Perez, H., and Imbrie, P., "In-situ strain measurements of EB-PVD thermal barrier coatings using synchrotron x-ray diffraction under thermo-mechanical loading," 49th AIAA Aerospace Sciences Meeting including the New Horizons Forum and Aerospace Exposition, 2011, p. 500.
- [8] Manero, A., Sofronsky, S., Knipe, K., Meid, C., Wischek, J., Okasinski, J., Almer, J., Karlsson, A. M., Raghavan, S., and Bartsch, M., "Monitoring local strain in a thermal barrier coating system under thermal mechanical gas turbine operating conditions," *JOM*, Vol. 67, No. 7, 2015, pp. 1528–1539.
- [9] Manero, A., Knipe, K., Wischek, J., Meid, C., Okasinski, J., Almer, J., Karlsson, A. M., Bartsch, M., and Raghavan, S., "Capturing the competing influence of thermal and mechanical loads on the strain of turbine blade coatings via high energy X-rays," *Coatings*, Vol. 8, No. 9, 2018, p. 320.
- [10] Stein, Z., Kenesei, P., Park, J.-S., Almer, J., Naraparaju, R., Schulz, U., and Raghavan, S., "High-energy X-ray phase analysis of CMAS-infiltrated 7YSZ thermal barrier coatings: Effect of time and temperature," *Journal of Materials Research*, ????, pp. 1–11.
- [11] Fouliard, Q., Hernandez, J., Heeg, B., Ghosh, R., and Raghavan, S., "Phosphor thermometry instrumentation for synchronized acquisition of luminescence lifetime decay and intensity on thermal barrier coatings," *Measurement Science and Technology*, Vol. 31, No. 5, 2020, p. 054007.
- [12] Rossmann, L., Northam, M., Sarley, B., Chernova, L., Viswanathan, V., Harder, B., and Raghavan, S., "Investigation of TGO stress in thermally cycled plasma-spray physical vapor deposition and electron-beam physical vapor deposition thermal barrier coatings via photoluminescence spectroscopy," Surface and Coatings Technology, Vol. 378, 2019, p. 125047.
- [13] Fouliard, Q., Ebrahimi, H., Hernandez, J., Vo, K., Accornero, F., McCay, M., Park, J.-S., Almer, J., Ghosh, R., and Raghavan, S., "Stresses within rare-earth doped yttria-stabilized zirconia thermal barrier coatings from in-situ synchrotron X-ray diffraction at high temperatures," *Surface and Coatings Technology*, Vol. 444, 2022, p. 128647.

[14] Naraparaju, R., Chavez, J. J. G., Schulz, U., and Ramana, C., "Interaction and infiltration behavior of Eyjafjallajökull, Sakurajima volcanic ashes and a synthetic CMAS containing FeO with/in EB-PVD ZrO2-65 wt% Y2 O3 coating at high temperature," *Acta Materialia*, Vol. 136, 2017, pp. 164–180.